Journal of Structural Geology 31 (2009) 853–856

Contents lists available at ScienceDirect

Journal of Structural Geology

journal homepage: www.elsevier.com/locate/jsg

Comment on "Structural controls on a carbon dioxide-driven mud volcano field in the Northern Apennines (Pieve Santo Stefano, Italy): Relations with pre-existing steep discontinuities and seismicity"

Cristiano Collettini*

Geologia Strutturale Geofisica, Dipartimento di Scienze della, Terra Università di Perugia, Piazza dell'Università 1, 06100 Perugia, Italy

ARTICLE INFO

Article history:
Received 12 December 2008
Received in revised form
17 February 2009
Accepted 18 February 2009
Available online 28 February 2009

Keywords
Fluid pressure
Fault reactivation analysis
Seismicity
Northern Apennines

ABSTRACT

Bonini (2009, Structural controls on a carbon dioxide-driven mud volcano field in the Northern Apennines (Pieve Santo Stefano, Italy): relations with pre-existing steep discontinuities and seismicity. Journal of Structural Geology 31, 44–54) presents a 2D mechanical analysis to infer the failure conditions responsible for the seismicity distribution during an $M_w = 4.6$ seismic sequence nucleating during 2001 in the Northern Apennines. In my view the mechanical analysis presented in this paper has some weakness or is not well constrained, in particular: 1) the assumption of a dip angle of 50°, is not consistent with the activated structures; 2) the $P_f = \sigma_3$ condition, difficult to be attained along a cohesionless fault dipping at 50°; 3) the isotropic stress state, i.e. $\sigma_2 = \sigma_3$, that is not consistent with the active or recent stress field in the area.

1. Introduction

In the 2D case where an existing fault, possessing friction equal to 0.6 (Byerlee, 1978) and containing the σ_2 axis, lies at a reactivation angle, θ_r, to σ_1, optimally oriented faults are located at $\theta_r \sim 30°$ (Sibson, 1985). As θ_r decreases or increases from this optimal orientation it is more and more difficult to reactivate a fault: well-oriented and misoriented faults lie in the range $30° < \theta_r < 45°$ and $45° < \theta_r < 60°$ respectively. Frictional lock-up is expected for $\theta_r \sim 60°$. In the field of severe misorientation, beyond frictional lock-up, fault reactivation is possible only when the tensile fluid pressure condition $P_f > \sigma_3$ is achieved (Sibson, 1985). The difficulty of maintaining the tensile fluid overpressure condition should prevent reactivation in the field of severely misoriented faults (Sibson, 1985; Collettini and Barchi, 2002). This mechanical analysis is consistent with the absence of moderate-to-large earthquake ruptures ($M > 5.5$) on low-angle normal faults (dip < 30°) where rupture plane is unambiguously discriminated (Collettini and Sibson, 2001).

From this brief introduction it is evident that the fault dip angle and the fluid pressure level are crucial considerations during any mechanical analysis.

2. Discussion on the mechanical analysis

2.1. The assumption of a dip angle of 50°

In Bonini (2009), an Anderson–Byerlee frictional fault reactivation model has been applied in order to explain the seismic events of the $M_w = 4.6$, San Sepolcro extensional seismic sequence. The author states that the seismic sequence occurred along the Altoriberina east-dipping low-angle normal fault, ATF (case 1). However in the conceptual model of Fig. 5b and Fig. 7a, the ATF is not shown and the fault that seems to play a key-role in controlling fluid flow, as a consequence of reactivation processes, is an SW-dipping normal fault bounding the eastern side of the Upper Tiber Basin, UTB (case 2).

In case 1, fault reactivation of the ATF, the dip angle of 50° is not consistent with: 1) the geometry of the mainshock focal mechanism showing a plane dipping at 21° eastward (Ciaccio et al., 2006); 2) the aftershock distribution highlighting a plane dipping in the range 20°–35° (Heinicke et al., 2006); 3) the geometry of the ATF at depths > 3 km as imaged by seismic reflection profiles, dip 15°–30° (Barchi et al., 1998); 4) the geometry of the ATF inferred by microseismicity, with a mean dip of ~15° (Chiaraluce et al., 2007).

In case 2, fault reactivation on the SW-dipping normal fault bounding the Upper Tiber Basin, the dip angle of 50° is consistent with the geometry of the fault mapped at the surface, but this fault was not reactivated during the 2001 seismic sequence, since all the

* Tel.: +39 (0)75 5867178; fax: +39(0)75 5852603.
E-mail address: colle@unipg.it

0191-8141/$ – see front matter © 2009 Elsevier Ltd. All rights reserved.
doi:10.1016/j.jsg.2009.02.002

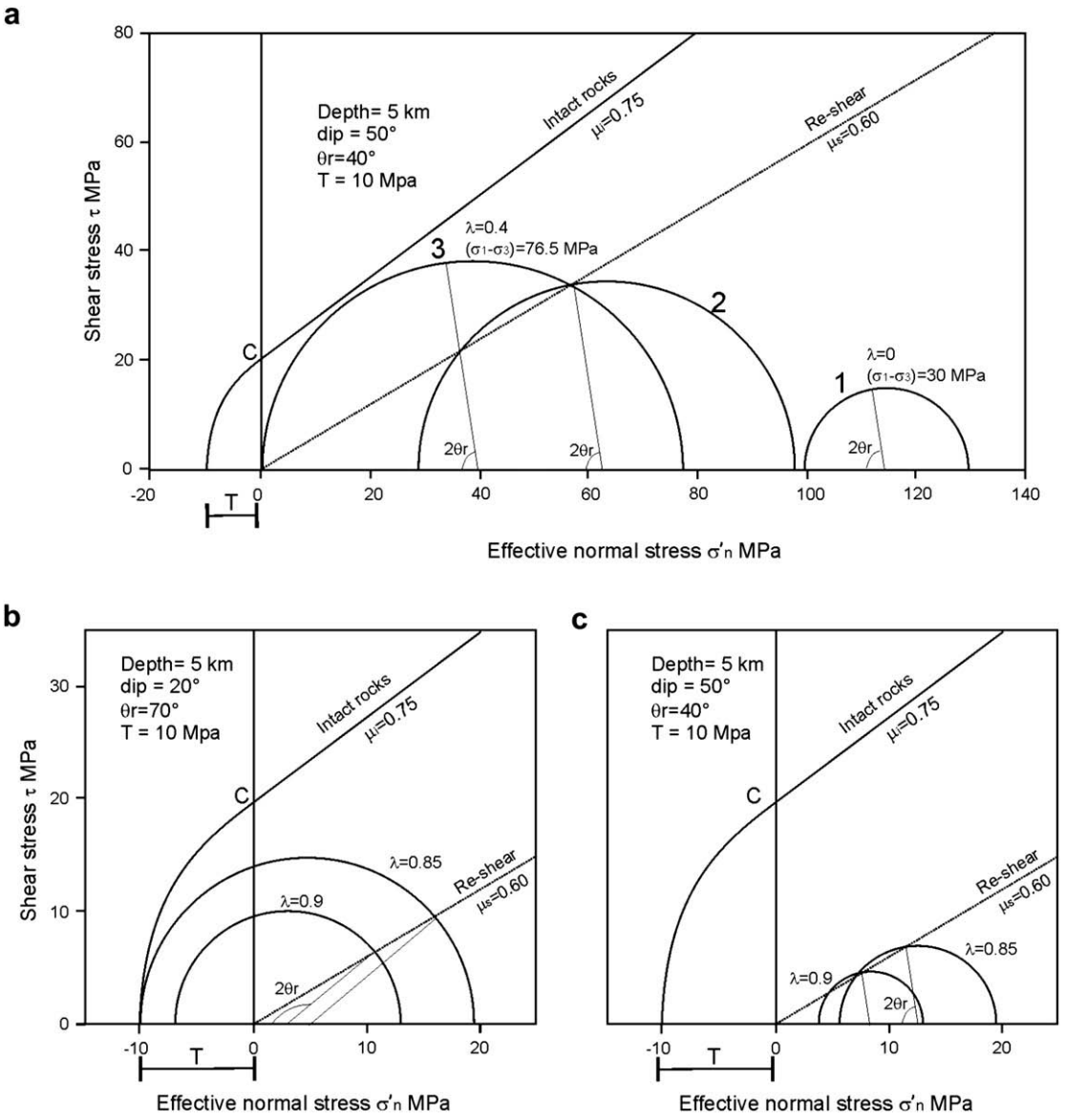

Fig. 1. (a) Composite Coulomb–Griffith diagram ($\mu_i = 0.75$; C = 20 MPa and T = 10 MPa) integrated with the re-shear condition ($\mu_s = 0.6$) of shear stress, τ, against effective normal stress, σ'_n. Starting from a stable state of stress, Mohr circle 1, $\lambda = 0$, $(\sigma_1 - \sigma_3) = 30$ MPa, during fault loading the reactivation of a fault dipping at 50° (e.g. Mohr circle 2) occurs before the attainment of the state of stress invoked in Bonini (2009), Mohr circle 3. Intact rock failure slope, μ_i, rock cohesion, C, rock tensile strength, T. (b) Differential stress $(\sigma_1 - \sigma_3)$, required for reactivation of the ATF, dip 20°, $\theta_r = 70°$, plotted in a composite Coulomb–Griffith diagram ($\mu_i = 0.75$; C = 20 MPa and T = 10 MPa) integrated with the re-shear condition ($\mu_s = 0.6$). Mohr circles are plotted for a pore fluid factor $\lambda = 0.9$ and 0.85. For $\lambda = 0.85$, the condition to form hydrofractures, $Pf = \sigma_3 + T$ is met. (c) Same boundary conditions as (b), but with a fault dip = 50° (e.g. Bonini, 2009). The Mohr circles have been constructed by using the script presented in Appendix 1.

earthquakes are located to the east of the surface expression of the fault and therefore the seismic activity cannot be related to an SW-dipping normal fault. Thus frictional fault reactivation cannot be applied to an SW-dipping normal fault, inclined at 50°, to explain the 2001 seismic sequence.

2.2. Mechanical analysis and the $P_f = \sigma_3$ condition

The mechanical analysis presented in Bonini (2009); Fig. 6, seeks to investigate the differential stress and fluid pressure conditions required for frictional reactivation of a cohesionless normal fault dipping at 50° ($\theta_r = 40°$, i.e. a well-oriented fault). The boundary conditions for the analysis are: vertical σ_1, intact rock failure slope, $\mu_i = 0.75$, friction coefficient $\mu_s = 0.6$, rock tensile strength, T = 10 MPa, z = 5 km. All the Mohr circles presented in Fig. 6 have a $\sigma'_3 = 0$, meaning that $P_f = \sigma_3$. My criticism here is that in the presence of a well-oriented cohesionless fault, the condition $\sigma'_3 = 0$ or $P_f = \sigma_3$ cannot be reached. To explain this I develop the same mechanical analysis presented in Bonini (2009) using the same equations and boundary conditions (Fig. 1 and Appendix 1 for a script used to reconstruct Mohr circles). Starting from a stable state of stress (Fig. 1, circle 1), in extensional environment, fault loading can occur by decreasing σ_3 and/or increasing fluid pressure, P_f. However during loading, whatever the increments in σ_3 or P_f, the Mohr circle intercepts the re-shear criterion (e.g. circle 2 in Fig. 1), well before reaching the condition $\sigma'_3 = 0$. The subsequent fault reactivation will create permeability with fluid pressure drops and therefore the Mohr circle is shifted to the right and it will be impossible to attain the state of stress represented by circle 3 (e.g. Bonini, 2009). In general, fracturing along well or optimally oriented faults creates permeability and prevents the attainment of fluid overpressures (e.g. Sibson, 2000; Townend and Zoback, 2000).

Fluid overpressure in the presence of a well-oriented fault can be attained if the fault has regained cohesion by cementation processes (Streit and Cox, 2001). In this case, however, Equations (1) and (2) reported in Bonini (2009) do not apply (cf. equations reported in Streit and Cox, 2001).

Collettini and Barchi (2002), for the same fault, presented the same mechanical analysis reported in Bonini (2009), but for the ATF dipping at 20°. The analysis suggests that the fault can be reactivated only under very restricted conditions, in general $P_f > \sigma_3$ or $\lambda > 0.85$ (Fig. 1b). This state of stress is equal, $\lambda = 0.85$, or more generally close, $\lambda > 0.85$, to the one required to form hydrofractures, i.e. $P_f = \sigma_3 + T$ (Secor, 1965). The tensile fluid pressure condition, $P_f > \sigma_3$, is difficult to sustain, and short-lived attainment of $P_f > \sigma_3$, due to CO_2 fluid overpressures has been invoked to explain the microseismicity along the ATF (Collettini and Barchi, 2002). I suggest that using the real geometry of the ATF, with a dip 20°–30° (Fig. 1b) instead of a dip of 50° (Bonini, 2009, Fig. 1c), the fault reactivation analysis points to a state of stress closer to the one invoked by Bonini (2009) to interpret part of the microseismicity as the result of hydrofracturing.

2.3. The isotropic stress state, i.e. $\sigma_2 = \sigma_3$

The seismicity occurred in December 2001, along the NE–SW Arbia-Val Marecchia Line, AVML, a right-lateral strike-slip structure, inherited from the previously developed phase of compressional tectonics. I agree that this seismicity occurs along the AVML and that it is the result of fluid-induced earthquakes during CO_2 discharge from a deep source. The geochemical and field data presented in Heinicke et al. (2006) and Bonini (2009) support this. However, I think that the interpretation of the earthquakes as NE–SW trending hydrofractures promoted by an isotropic state of stress in the horizontal plane, i.e. $\sigma_2 = \sigma_3$ (Bonini, 2009), is unlikely. I think that the condition $\sigma_2 = \sigma_3$ is not consistent with the active or recent state of stress in the Northern Apennines. First, the orientation of active faults mapped at the surface (Barchi, 2000) and stress inversions on small displacement striated fault surfaces (e.g. Lavecchia et al., 1994; Boncio et al., 2000; Bonini, 2009, Fig. 5) show a state of stress that is clearly anisotropic in the horizontal plane. Second, GPS data show a constant NW–SE trending extensional rate of 2.5–3.5 mm/yr (Hunstad et al., 2003). Third, the focal mechanisms of the major earthquakes of the area (Chiaraluce et al., 2003; Ciaccio et al., 2006) are consistent with an anisotropic state of stress.

For the AVML I suggest a different mechanical interpretation on the basis of experience gained during another seismic sequence occurring in the same portion of the Northern Apennines, the Colfiorito 1997–1998 sequence (Chiaraluce et al., 2003). The Colfiorito sequence, like San Sepolcro, occurred on NW-trending normal fault and the two main ruptures are segmented by an NNE–SSW trending, right-lateral strike-slip fault inherited from the compressional phase (Chiaraluce et al., 2003; Collettini et al., 2005). Late in the Colfiorito seismic sequence, this strike-slip fault nucleated a left-lateral strike-slip mainshock and an associated aftershock sequence with left-lateral strike-slip focal mechanisms. Static stress change analysis shows that elastic stress perturbations induced by the occurrence of normal fault earthquakes promoted the reactivation of the strike-slip structure with left-lateral kinematics (Collettini et al., 2005). In addition, the left-lateral sense of shear along the NNE–SSW trending structure is favoured by the orientation of the fault relative to the NE–SW trending regional extension direction (Collettini et al., 2005). Following the experience of Colfiorito 1997–1998, I therefore suggest that the earthquakes along the AVML can be interpreted as fluid-driven, fault reactivation processes along a pre-existing steeply dipping NE–SW trending structure inherited from the earlier compressional tectonic phase.

Appendix. 1

% Matlab script to plot in a composite Coulomb–Griffith diagram integrated with the re-shear condition Mohr circles that represent 2D frictional reactivation along a fault with a specific dip.

```
clear
clf
A = 40;                          %reactivation angle in degrees
teta = (2*pi*A)/360;             %from degrees to radiant
rho = 2600;                      %density of the crust (kg/m^3)
g = 9.8                          %gravitational acceleration (m/s^2)
z = 5000                         %focal depth in m
mu = 0.6                         %sliding friction coefficient%
lambda = 0.4;                    %pore fluid factor%
```

$$DifS = (1 - mu*\tan(teta))./(1 + mu*\cot(teta))* rho*g*z*(1 - lambda)$$

%Equation (2) in Bonini (2009) after Sibson (2000).

$$DifS = (\tan(teta) + \cot(teta))./(1 + mu*\cot(teta))* mu*rho*g*z*(1 - lambda)$$

%Equation (1) in Bonini (2009) after Sibson (2000).

```
%Parametric equation of a circle%
a = Sp3 + DifS/2                 %a centre of the Mohr circle
r = DifS/2                       %radius of the Mohr circle
A = 0:1:90;
alfa = (2*pi*A)/360;
x = a - r*cos(2*alfa)
y1 = r*sin(2*alfa)
plot(x,y1,'r')
hold on
```

```
%Coulomb's criterion
C = 20 000 000                   %cohesion of the rocks C = 2T in Pa%
mui = 0.75                       %internal friction coefficient%
x = 0:100 000:80 000 000
y2 = C + mui*x
plot(x,y2)
hold on
```

```
%reactivation criterion or Amonton law
x = 0:100 000:80 000 000
y3 = mu*x
plot(x,y3)
hold on
```

```
%Griffith's criterion%
T = 10 000 000                   %tensile strength of the rocks in Pa%
x = -12 000 000:100 000:0
y4 = sqrt(4*T*x + 4*T.^2)
plot (x,y4)
axis equal
```

References

Barchi, M.R., Minelli, G., Pialli, G., 1998. The crop 03 profile: a synthesis of results on deep structures of the Northern Apennines. Mem. Soc. Geol. It. 52, 383–400.

Barchi, M. R., Galadini, F., Lavecchia, G., Messina, P., Michetti, A. M., Peruzza, L., Pizzi, A., Tondi, E., Vittori, E., 2000. Sintesi sulle conoscenze delle faglie attive in Italia Centrale. Gruppo Nazionale per la Difesa dei Terremoti.

Boncio, P., Brozzetti, F., Lavecchia, G., 2000. Architecture and seismotectonics of a regional low-angle normal fault zone in central Italy. Tectonics 19, 1038–1055.

Bonini, M., 2009. Structural controls on a carbon dioxide-driven mud volcano field in the Northern Apennines (Pieve Santo Stefano, Italy): relations with pre-existing steep discontinuities and seismicity. J. Struct. Geol. 31, 44–54.
Byerlee, J.D., 1978. Friction of rocks. Pure Appl. Geophys. 116, 615–626.
Chiaraluce, L., Ellsworth, W.L., Chiarabba, C., Cocco, M., 2003. Imaging the complexity of an active normal fault system: the 1997 Colfiorito (Central Italy) case study. J. Geophys. Res. 108 (B6), 2294, doi:10.1029/2002JB002166.
Chiaraluce, L., Chiarabba, C., Collettini, C., Piccinini, D., Cocco, M., 2007. Architecture and mechanics of an active low-angle normal fault: Alto Tiberina Fault, northern Apennines, Italy. J. Geophys. Res. 112 (B10310), doi:10.1029/2007JB005015.
Ciaccio, M.G., Pondrelli, S., Frepoli, A., 2006. Earthquake fault-plane solutions and patterns of seismicity within the Umbria Region, Italy. Ann. Geophys. 29, 987–1002.
Collettini, C., Barchi, M.R., 2002. A low angle normal fault in the Umbria region (Central Italy): a mechanical model for the related microseismicity. Tectonophysics 359, 97–115.
Collettini, C., Chiaraluce, L., Pucci, S., Barchi, M.R., Cocco, M., 2005. Looking at fault reactivation matching structural geology and seismology. J. Struct. Geol. 5, 937–942.
Collettini, C., Sibson, R.H., 2001. Normal faults normal friction? Geology 29, 927–930.
Heinicke, J., Braun, Y., Burgassi, P., Italiano, F., Martinelli, G., 2006. Gas flow anomalies in seismogenic zones in the Upper Tiber Valley, Central Italy. Geophys. J. Int. 167, 794–806.
Hunstad, I., Selvaggi, G., D'Agostino, N., England, P., Clarke, P., Pierozzi, M., 2003. Geodetic strain in peninsular Italy between 1875 and 2001. Geophys. Res. Lett. 30 (4), 1181, doi:10.1029/2002GL016447.
Lavecchia, G., Brozzetti, F., Barchi, M.R., Keller, J.V.A., Menichetti, M., 1994. Seismotectonic zoning in east-central Italy deduced from the analysis of the Neogene to present deformations and related stress fields. Geol. Soc. Am. Bull. 106, 1107–1120.
Secor, D.T., 1965. Role of fluid pressure in jointing. Am. J. Sci. 263, 633–646.
Sibson, R.H., 1985. A note on fault reactivation. J. Struct. Geol. 7, 751–754.
Sibson, R.H., 2000. Fluid involvement in normal faulting. J. Geodyn. 29, 469–499.
Streit, J.E., Cox, S.F., 2001. Fluid pressures at hypocenters of moderate to large earthquakes. J. Geophys. Res. 106 (B2), 2235–2243.
Townend, J., Zoback, M.D., 2000. How faulting keeps the crust strong. Geology 28, 399–402.